ChemComm
Chemical Communications

Accepted Manuscript

This article can be cited before page numbers have been issued, to do this please use: C. wu, S. Wang, X. Luo, R. Yuan and X. Yang, *Chem. Commun.*, 2020, DOI: 10.1039/C9CC08440A.

ROYAL SOCIETY OF CHEMISTRY

rsc.li/chemcomm

ROYAL SOCIETY OF CHEMISTRY View Article Online
DOI: 10.1039/C9CC08440A

Journal Name

COMMUNICATION

Adenosine Triphosphate Responsive Metal–organic Frameworks Equipped with DNA Structure Lock for Construction of Ratiometric SERS Biosensor

Received 00th January 20xx,
Accepted 00th January 20xx

DOI: 10.1039/x0xx00000x
www.rsc.org/

Caijun Wu[1], ShufanWang[1], Xiliang Luo[2], Ruo Yuan*[1], Xia Yang*[1]

A novel ratiometric surface-enhanced Raman scattering (SERS) biosensor was constructed based on stimuli-responsive DNA functionalized metal organic frameworks (MOFs) for detection of adenosine triphosphate (ATP). As a result, the detection range of ATP was 1 nM to 200 nM with detection limit of 0.4 nM. The ratiometric SERS biosensor strategy offers lower detection limit and more excellent performance than the typical SERS detection based on single signal response, which may have potential for detection of other biomoleculars or metal ions.

Adenosine triphosphate (ATP) [1], the most direct energy source in the organism, plays a crucial role in the storage, transfer of energy and the synthesis of nucleic acids. Nonetheless, abnormal ATP levels in the body are usually associated with cardiovascular diseases, cancers, Parkinson's disease and etc.[2,3] Surface enhanced Raman scattering (SERS) has been widely used for quantitative detection of DNA,[4] RNA,[5] proteins[6] and other biological molecules owing to the high sensitivity, nondestructive detection and unique Raman fingerprint.[7, 8] SERS substrate was an important factor for SERS quantification[9, 10]. By far, noble metal nanoparticles with various shapes were served as SERS substrate, such as nanospheres,[11] nanocages,[12] nanorods[13] and nanothons.[14] In this work, gold nanoflowers (GNFs) was employed as the SERS substrate because the surface area of GNFs petals were much larger than that of nanospheres, and the sharp edge of GNFs petals can enhance electromagnetic fields to improve the SERS intensity significantly.[15]

Traditional SERS biosensors often employed one Raman signal to quantitatively analyze the targets, which limited the reliability of SERS detection due to the uncontrollable environmental factors, including the laser power and the focal length.[16, 17] In order to solve the problems, internal standard or ratiometric method was often introduced in the SERS system,[18] which could reduce the interference of background and improved the reliability of SERS biosensor remarkably. Recently, our group had constructed a ratiometric SERS sensor with DNA hydrogel-captured glucose oxidase in the preliminary work.[19] However, the intensity ratio of the two Raman signals needed to be further improved to enhance the sensitivity of the biosensor. In this work, the intensity ratio of the two Raman signals was significantly amplified to enhance the sensitivity of the biosensor.

Nowadays, metal organic frameworks (MOFs) are often widely applied in gas storage,[20] organic matter adsorption,[21] metal ions detection,[22] protein detection[23] due to their large specific surface area, highly ordered topological structure, excellent biocompatibility and high porosity.[24-26] Recently, MOFs were emerged as the carrier materials for constructing biological platform.[27-29] Most representatively, Willner et al. had assembled a series of stimuli-responsive DNA-functionalized MOFs as the drug carriers in cancer cells.[30] O. Farha et al. had synthesized Zr-MOF as a nanosized enzyme carriers for accelerating hydrolysis of nerve agent.[31] In this study, the DNA functionalized MOFs were employed for loading Raman molecule (TB) inside. In the presence of ATP, the DNA structure on the surface of the MOFs was disassembled to

1 Key Laboratory of Luminescent and Real-Time Analytical Chemistry (Southwest University), Ministry of Education; College of Chemistry and Chemical Engineering, Southwest University, Chongqing, PR China
2 Shandong Key Laboratory of Biochemical Analysis; College of Chemistry and Molecular Engineering, Qingdao University of Science and Technology, Qingdao 266042, PR China
Corresponding author. Tel.: +86-23-68252277; Fax: +86-23-68253172
E-mail address: yuanruo@swu.edu.cn (R. Yuan); xiayang2@swu.edu.cn(X. Yang)
Electronic Supplementary Information (ESI) available: Experimental details, material characterizations and performance of biosensor. See DOI: 10.1039/x0xx00000x

View Article Online
DOI: 10.1039/C9CC08440A

release toluidine blue (TB) and complementary DNA (cDNA) for obtaining the Raman signal of TB.

In this strategy, a SERS biosensor was fabricated based on the DNA structure functionalized MOFs. Firstly, TB was encapsulated in the micropores by modifying DNA Y-junction on the surface of MOFs.[32, 33] The ternary Y-junction was consisted of ATP aptamer (S2), cDNA and single strained DNA (S1). As shown in scheme 1, in the presence of ATP, the ATP aptamer combined with ATP to disintegrate the Y-junction structure, so large amount of TB and cDNA were released. After that, when the solution containing TB and cDNA was dropped on the GNFs with hairpin DNA (H1), the cDNA complemented with H1 (labeled by Cy5) to form the rigid double-stranded DNA (dsDNA) on the substrate. As a result, TB was adsorbed on the SERS substrate to insert into the dsDNA for increasing TB Raman intensity (I_{TB}). Meanwhile, the formation of the dsDNA made Cy5 far from the substrate, causing the decrease of the Cy5 Raman intensity (I_{Cy5}). Based on the above principle, with the augmenting concentration of ATP, the ratio of I_{TB}/I_{Cy5} would increase, and thus a ratiometric biosensor for detection of ATP was constructed. This proposed SERS platform had good performance for trace detection of ATP, which may give a new strategy for diagnosis of other biomolecular.

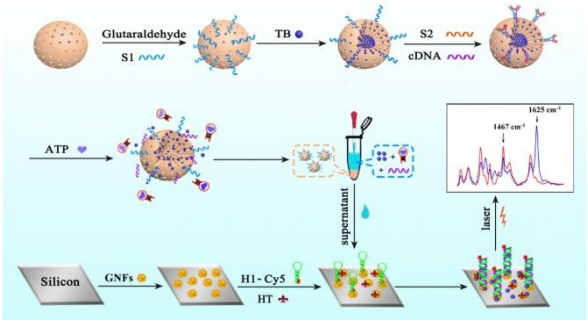

Scheme 1. The construction process of SERS biosensor for ATP detection.

To prove that TB was successfully blocked in the MOFs by the DNA ternary Y-junction, we measured the UV-vis absorption spectrums of MOF@TB and MOF@TB@Y-junction. As shown in Figure 1A, when TB was encapsulated in the micropores by modifying Y-junction on the surface of MOFs (MOF@TB@Y-junction), the absorbance intensity sharply declined compared to that of MOF@TB without Y-junction, which showed that TB was encapsulated in the MOFs. In addition, the UV-vis absorption spectrums of MOFs@TB@Y-junction in ultra-pure water after 0.5, 6, 12 and 24 hours were shown in Figure 1C, respectively. We can see that the absorbance intensity has no significant change for a long time, which indicated that the MOFs@TB@Y-junction owned good stability in water without TB leakage. And we employed polyacrylamide gel electrophoresis (PAGE) to evaluate the formation of DNA ternary Y-junction (Figure 1B). The distinct bands observed in lane b, lane c and lane d represented the single-stranded DNA of S1, S2 and complementary DNA (cDNA). After rapid solution annealing of the three DNA strands, a band with very low mobility was observed in lane e, illustrating the successful formation of DNA ternary Y-junction.

The SERS signal response of ATP was collected by Raman spectrometer with a 633 nm laser. The typical Raman peaks at 1625 cm^{-1} of TB and 1467 cm^{-1} of Cy5 can be used as the characteristic peaks of Raman response of ATP. Figure 1D displayed the supernatant of MOF@TB@Y-junction had a weak Raman response on the GNFs (without H1-Cy5) (curve a), which was caused by the nonspecific adsorption between TB and MOFs. With the existence of ATP (1 μM), the Raman signal of the supernatant on the GNFs (without H1-Cy5) increased significantly (curve b). More importantly, an obvious color change was seen before and after the release of TB by adding ATP as shown in Figure 1E. In Figure 1F, when H1-Cy5 still maintained a hairpin structure on the GNFs, Cy5 was closest to the GNFs and the biosensor had the strongest Raman signal of Cy5 at 1467 cm^{-1} (curve a). When 1 μM ATP was added, the DNA Y-junction was destroyed and the dsDNA-GNFs conjugates (H1 and cDNA) were formed on the SERS substrates. Then Cy5 was far from the GNFs and the I_{Cy5} reduced, and TB was adsorbed on the SERS substrate to insert into the dsDNA, resulting in the enhancement of I_{TB} (curve b) at 1625 cm^{-1}.

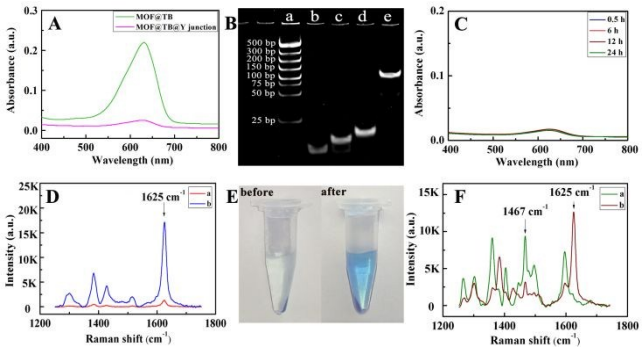

Figure 1. (A) The UV-vis absorption spectrums of MOF@TB and MOF@TB@Y-junction. (B) PAGE analysis of DNA ternary Y-junction. Lanes a-e represent DNA marker, S1, S2, cDNA, DNA Y-junction. (C) The UV-vis absorption spectrums of MOF@TB@Y-junction in pure water after 0.5, 6, 12 and 24 hours. (D) SERS spectra of the supernatant of MOFs@TB@Y-junction solution on the GNFs surface (without H1-Cy5)(curve a). SERS spectra of the supernatant of MOFs@TB@Y-junction solution in the presence of ATP (1 μM) on the GNFs surface (without H1-Cy5) (curve b). (E) The color

View Article Online
DOI: 10.1039/C9CC08440A

contrast of solution before and after TB releasing. (F) SERS spectra after Cy5 labeled H1 was fixed on the GNFs surface (curve a). SERS spectra after the releasing supernatant was dropped onto the GNFs@H1 surface (curve b).

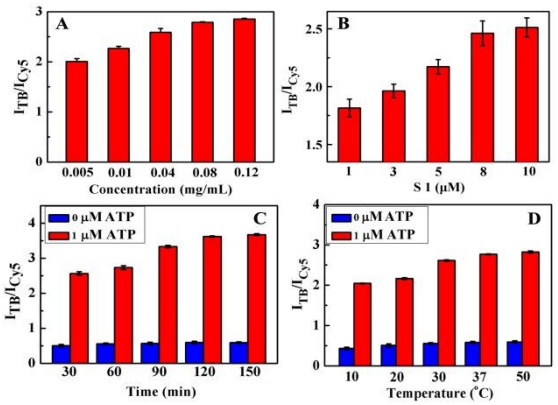

Figure 2. I_{TB}/I_{Cy5} values of the SERS biosensor (A) with different concentrations of TB, (B) different concentrations of S1, (C) with different incubation times of ATP (1 μM) and (D) with different incubation temperatures of ATP (1 μM). (the blue bars indicate the absence of ATP and the red indicate the presence of ATP (1μM).)

We optimized the experimental conditions, including concentration of TB, different concentrations of S1, incubation time and incubation temperature of ATP for further promoting the sensitivity of the biosensor. The SERS signal response was investigated after incubated with various TB concentrations. Figure 2A exhibited that the loading of TB by MOFs almost reached saturation with the increasing concentrations of TB, and the optimal concentration of TB was 0.08 mg/mL. In addition, we have optimized the amount of S1 for further promoting the sensitivity of the biosensor. Different concentrations of S1 solutions of 1, 3, 5, 8, 10 μM were firstly prepared. Figure 2B displayed the I_{TB}/I_{Cy5} values corresponding to various concentration of S1 after incubated with 1μM ATP. We can see that the I_{TB}/I_{Cy5} values increased gradually along with increasing concentration of S1. Therefore, 10 μM of S1 was selected in the experimental system. And the incubation time of ATP (1 μM) had a significant influence on the level of TB release. From Figure 2C, it could be seen that the changes of I_{TB}/I_{Cy5} value under different incubation times and it reached equilibrium when the incubation time of ATP was 120 minutes. What's more, the incubation temperature of ATP was also studied. From Figure 2D, we can see that after 37 °C, the SERS intensity tended to be stable, so 37 °C was chosen as the optimal temperature for incubation of ATP. The blue bars in Figure 2C and 2D indicated the I_{TB}/I_{Cy5} values had no significant change with the absence of ATP under different incubation times and incubation temperatures of ATP.

On the basis of the optimum conditions, we explored the Raman response of the SERS platform after incubation with different concentrations of ATP from 1 nM to 50 μM (n = 3). From Figure 3A and 3B, with the gradually increasing of the concentration of ATP, the Raman signal of Cy5 decreased at 1467 cm^{-1} and TB increased at 1625 cm^{-1} with the increasing of ATP concentration continuously. I_{TB}/I_{Cy5} values were used as the quantitative criteria to study the detection of ATP. Figure 3C depicted the ATP concentration-dependent I_{TB}/I_{Cy5} values changes. Figure 3D showed an accurate linear relationship between I_{TB}/I_{Cy5} values and ATP from 1 nM to 200 nM. And the linear regression equation was y = 1.342 + 0.00527c (R^2 = 0.998), where y represented the I_{TB}/I_{Cy5} value and c equated with the concentration of ATP. The limit of detection (LOD) was calculated as 0.4 nM. The LOD was calculated as LOD = $3S_b$ / m,[34] where S_b is the standard deviations of the SERS signals for blank samples (n_b = 11) and m is the slope of the corresponding linear regression equation. From Table S2, our proposed SERS based strategy had an excellent sensitivity to detect ATP compared to other biosensors in the literature.

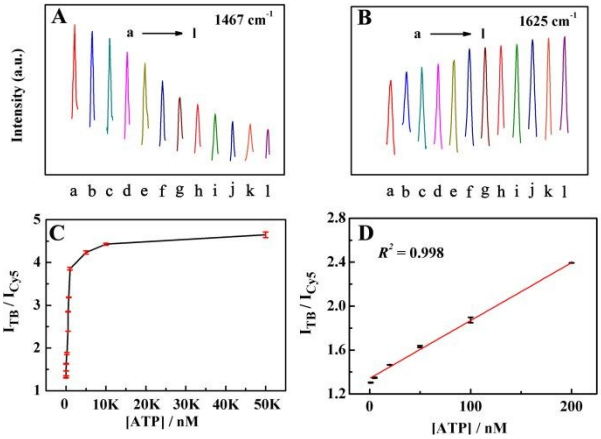

Figure 3. The variation trend of Raman intensity of (A) Cy5 and (B) TB with the increasing trend of the elevated concentration of ATP (nM) from a to l: (a) 1, (b) 5, (c) 20, (d) 50, (e) 100, (f) 200, (g) 500, (h) 700, (i) 1000, (j) 5000, (k) 10000, (l) 50000. (C) The I_{TB}/I_{Cy5} values with different ATP concentrations. (D) The calibration curve of I_{TB}/I_{Cy5} values and ATP concentration (error bars = RSD, n = 3).

In summary, our results further demonstrated that a ratiometric SERS sensor based MOFs was successfully constructed, which had a ATP detection range from 1 nM to 200 nM with detection limit of 0.4 nM. The SERS platform utilized DNA ternary Y-junction to block TB in the porous MOFs. When the concentration of ATP was increasing, the ratio of I_{TB}/I_{Cy5} value changed significantly to amplify SERS signal. So the SERS biosensor combined the porous MOFs and DNA technology can have a sensitive detection of ATP, which may broaden the application and improve the feasibility of the SERS related bioanalysis.

Conflicts of interest

There are no conflicts to declare.

Acknowledgements

This work was supported by the NNSF of China (51602263), the Chongqing Research Program of Basic Research and Frontier Technology (cstc2019jcyj-msxmX0209), the Fundamental Research Funds for the Central Universities (XDJK2019C077), Open Project Program from College of Chemistry and Molecular Engineering, Qingdao University of Science and Technology (QUSTHX201804). The authors also thank Xia Zhong (Southwest University) for the Raman technical support.

Notes and references

1. Y.-Y. Fan, Z.-L. Mou, M. Wang, J. Li, J. Zhang, F.-Q. Dang and Z.-Q. Zhang, *Anal. Chem.*, 2018, **90**, 13708-13713.

2. Y. Peng, D. Li, R. Yuan and Y. Xiang, *Biosens. Bioelectron.*, 2018, **105**, 1-5. Biosensors and Bioelectronics, 2018, 105, 1-5.

3. X. Zheng, R. Peng, X. Jiang, Y. Wang, S. Xu, G. Ke, T. Fu, Q. Liu, S. Huan and X. Zhang, *Anal. Chem.*, 2017, **89**, 10941-10947.

4. S. Tian, O. Neumann, M. J. McClain, X. Yang, L. Zhou, C. Zhang, P. Nordlander and N. J. Halas, *Nano Lett.*, 2017, **17**, 5071-5077.

5. M. Q. He, S. Chen, K. Yao, K. Wang, Y. L. Yu and J. H. Wang, *Small Methods*, 2019, **3**, 1900017.

6. Y. Chen, D. Ni, X. Yang, C. Liu, J. Yin and K. Cai, *Electrochim. Acta*, 2018, **278**, 114-123.

7. D. Sun, F. Cao, W. Xu, Q. Chen, W. Shi and S. Xu, *Anal. Chem.*, 2019, **91**, 2551-2558.

8. X. Wang, W. Shi, S. Wang, H. Zhao, J. Lin, Z. Yang, M. Chen and L. Guo, *J. Am. Chem. Soc.*, 2019, **141**, 5856-5862.

9. Y. Yang, J. Zhu, J. Zhao, G.-J. Weng, J.-J. Li and J.-W. Zhao, *ACS Appl. Mater. Inter*, 2019, **11**, 3617-3626.

10. X. Wang, G. Ma, A. Li, J. Yu, Z. Yang, J. Lin, A. Li, X. Han and L. Guo, *Chem. Sci.*, 2018, **9**, 4009-4015.

11. K. Liu, Y. Bai, L. Zhang, Z. Yang, Q. Fan, H. Zheng, Y. Yin and C. Gao, *Nano Lett.*, 2016, **16**, 3675-3681.

12. M. Kim, S. M. Ko, C. Lee, J. Son, J. Kim, J. M. Kim and J. M. Nam, *Anal. Chem.*, 2019, **91**, 10467-10476.

13. J. Zhou, J. Zhang, H. Yang, Z. Wang, J.-a. Shi, W. Zhou, G. Xian, Q. Qi, Y. Weng and N. Jiang, *Nanoscale*, 2019,**11**, 11782-11788.

14. B. Yang, D. Bin, K. Zhang, Y. Du and T. Majima, *J. Colloid Interf. Sci.*, 2018, **512**, 446-454.

15. M. Bardhan, B. Satpati, T. Ghosh and D. Senapati, *J. Mater. Chem. C*, 2014, **2**, 3795-3804.

View Article Online
DOI: 10.1039/C9CC08440A

16. Y. Chen, Z.-P. Chen, S.-Y. Long and R.-Q. Yu, *Anal. Chem.*, 2014, **86**, 12236-12242.

17. K. Zhang, Y. Wang, M. Wu, Y. Liu, D. Shi and B. Liu, *Chem. Sci.*, 2018, **9**, 8089-8093.

18. Y. Zhao, F. Zheng, W. Ke, W. Zhang, L. Shi and H. Liu, *Anal. Chem.*, 2019, **91**, 7162-7172.

19. Y. He, X. Yang, R. Yuan and Y. Chai, *J. Mater. Chem. B*, 2019, **7**, 2643-2647.

20. H. Li, K. Wang, Y. Sun, C. T. Lollar, J. Li and H.-C. Zhou, *Mater. Today*, 2018, **21**, 108-121.

21. Z. Hasan and S. H. Jhung, *J. Hazard. Mater.*, 2015, **283**, 329-339.

22. P. Samanta, A. V. Desai, S. Sharma, P. Chandra and S. K. Ghosh, *Inorg. Chem.*, 2018, **57**, 2360-2364.

23. Z. Wang, P. Dong, Z. Sun, C. Sun, H. Bu, J. Han, S. Chen and G. Xie, *J. Mater. Chem. B.* 2018b. **6(16)**, 2426-2431.2018.

24. M. Ding, R. W. Flaig, H.-L. Jiang and O. M. Yaghi, *Chem. Soc. Rev.*, 2019, **48**, 2783-2828.

25. M. Nasalevich, M. Van der Veen, F. Kapteijn and J. Gascon, *CrystEngComm*, 2014, **16**, 4919-4926.

26. C. S. L. Koh, H. K. Lee, X. Han, H. Y. F. Sim and X. Y. Ling, *Chem. Commun.*, 2018, **54**, 2546-2549.

27. Z. Wang, B. Ma, C. Shen and L. Z. Cheong, *Talanta*, 2019, **197**, 356-362.

28. W.-H. Chen, X. Yu, W.-C. Liao, Y. S. Sohn, A. Cecconello, A. Kozell, R. Nechushtai and I. Willner, *Adv. Funct. Mater.*, 2017, **27**, 1702102.

29. X. Kuang, S. Ye, X. Li, Y. Ma, C. Zhang and B. Tang, *Chem. Commun.*, 2016, **52**, 5432-5435.

30. J. S. Kahn, L. Freage, N. Enkin, M. A. Garcia and I. Willner, *Adv. Mater.*, 2017, **29**, 1602782.

31. P. Li, S. Y. Moon, M. A. Guelta, L. Lin, D. A. Gomez-Gualdron, R. Q. Snurr, S. P. Harvey, J. T. Hupp and O. K. Farha, *ACS Nano*, 2016, **10**, 9174-9182.

32. P. Zhang, X. Wu, R. Yuan and Y. Chai, *Anal. Chem.*, 2015, **87**, 3202-3207.

33. S. Tang, P. Tong, H. Li, F. Gu and L. Zhang, *Biosens. Bioelectron.*, 2013, **41**, 397-402.

34. Y. He, X. Yang, R. Yuan and Y. Chai, *Anal. Chem.*, 2017, **89**, 8538-8544.